Philosophical Magazine A, 2002, Vol. 82,
No. 17/18, 3383–3391

Taylor & Francis
Taylor & Francis Group

Fiducial mark and nanocrack zone formation during thin-film delamination

Alex A. Volinsky†‖, Neville R. Moody‡, Michael L. Kottke† and William W. Gerberich§

† Motorola, Digital DNA™ Laboratories, Process and Materials Characterization Laboratory, Mesa, Arizona 85202, USA
‡ Sandia National Laboratories, Livermore, California 94551, USA
§ University of Minnesota, Department of Chemical Engineering and Materials Science, Minneapolis, Minnesota 55455, USA

Abstract

Carbon fiducial marks are formed during thin-film local delamination processes induced either by superlayer indentation forming circular blisters, or by residual stress relief through telephone cord blister formation. Hydrocarbons are sucked into the crack tip during the delamination process, outlining the crack-tip-opening angle, which can be used to back calculate thin-film adhesion using either elastic or plastic analyses presented here. Fiducial marks have been observed in two different thin-film systems, namely Cu/SiO_2 and TiW_xN_y/GaAs. Cu/SiO_2 delamination blisters have been cross-sectioned using the focused-ion-beam method, and high-resolution scanning electron microscopy of the cross-sections revealed crack renucleation ahead of the original crack tip. This is attributed to the stress redistribution process due to the dislocation shielding mechanism. At stress intensity levels of $0.33\,MPa\,m^{1/2}$, it is found that four emitted dislocations can account for crack arrest, with renucleation of 100 nm sized nanocracks dependent on the antishielding stresses.

§1. Introduction

There are several different methods available to measure thin-film adhesion quantitatively (Marshall and Evans 1984, Vlassak and Nix 1992, Bagchi *et al.* 1994, Bugchi and Evans 1995, Vlassak *et al.* 1997, Dauskardt *et al.* 1998, Sanchez *et al.* 1999). A review of testing techniques primarily applicable to ductile films has been given by Volinsky *et al.* (2002b). One of the ways of measuring ductile thin-film adhesion is by means of the superlayer indentation technique (Gerberich *et al.* 1999, Kriese and Gerberich 1999, Kriese *et al.* 1999, Volinsky *et al.* 1999a, b, Tymiak *et al.* 2000). This is similar to the single-layer indentation test originally developed by Marshall and Evans (1984) and extended for multilayers by Kriese and Gerberich (1999). Most well-adhered thin films cannot be delaminated by means of regular single-layer indentation; ductile films would rather deform plastically around the indenter by forming a pile-up. To prevent these problems a high-modulus hard superlayer (e.g. tungsten, TiW or Ta_2N), capable of supporting and storing large amounts of elastic energy is deposited on top of the film of interest. Upon indentation a delamination blister forms around the indent (see figure 1), and

‖ Email: Alex.Volinsky@motorola.com

Philosophical Magazine A ISSN 0141–8610 print/ISSN 1460-6992 online
http://www.tandf.co.uk/journals
DOI: 10.1080/01418610210150622

its area is used to calculate the strain energy release rate (practical work of adhesion). This technique was shown to work with ductile metallic films (aluminium, copper, gold and chromium) (Schneider *et al.* 1998, 1999, Kriese and Gerberich 1999, Kriese *et al.* 1999, Volinsky *et al.* 1999b, 2000, Moody *et al.* 2000, Tymiak *et al.* 2000), ceramic (Ta_2N) (Moody *et al.* 1997, 1998b) and polymer films (Volinsky *et al.* 2002c).

While ductile thin-film adhesion increases with increasing film thickness owing to the increased plasticity contributions (Dauskardt *et al.* 1998, Volinsky *et al.* 1999a, b, 2000, 2002b), a brittle-to-ductile transition was found in copper thin films on silicon substrates that occurs on decreasing the film thickness below 120 nm (Volinsky *et al.* 1999b, 2002b, Tymiak *et al.* 2000). Temperature effects on the brittle-to-ductile transition have also been discussed by Gerberich *et al.* (2000) and Volinsky *et al.* (2002b).

During indentation experiments into copper thin films with a tungsten superlayer it was found that crack arrest (fiducial) marks form and correspond exactly to the blister size (Volinsky 1999b). Marks are formed of carbon and outline the crack tip, representing its geometry (Volinsky *et al.* 1999a, b, 2002a). Given the transition, the following elastic and plastic analyses demonstrate how such marks can be used as a measure of fracture resistance. Furthermore, for the relatively thin film analysed, it will be shown that the very low toughness found on the lower shelf of the brittle-to-ductile transition implies nearly negligible plasticity. This is reinforced by a dislocation shielding interpretation of a nanocrack process zone found at the leading edge of the delamination front.

§ 2. Fiducial marks

Fiducial crack arrest marks were found after the blister removal with an adhesive tape. Scanning electron microscopy (SEM) showed circles that correspond to the original blister diameter, and those were denoted as crack arrest fiducial marks (Volinsky *et al.* 1999a, b, 2002a). Atomic force microscopy (AFM) was performed to measure the feature geometry, giving a width over 1 μm, and a height ranging from 5 to 15 nm. Deflection AFM and SEM images of the partially removed blister showing the fiducial crack arrest marks are presented in figure 1.

There are three possible sources for carbon: adhesive tape, the diamond indenter and hydrocarbons from the atmosphere. In our previous studies the first two sources were eliminated (Volinsky *et al.* 1999a, b), and hydrocarbons from the atmosphere were proposed as a source of fiducial mark formation.

In the case of a compressed film, residual stresses can be relieved through local film delamination immediately followed by buckling, forming the classic telephone cord delamination patterns. During the course of this study it was found that a similar type of carbon contamination is present in a different film system of Ti_xWN_y on GaAs, where the telephone cord delaminations formed owing to the high compressive residual stress relief (figure 2). The carbon traces noted on both the film and the substrate surfaces mimic the original telephone cord delamination pattern, except that the cause of initial thin-film delamination is different in this case. Fiducial crack arrest marks are like those observed in the Cu/SiO_2 system. Figure 2 also shows a carbon Auger map, where brighter areas correspond to higher carbon concentrations. There is almost no carbon present between the original telephone cord delaminated areas (black regions in figure 2), which were exposed to air

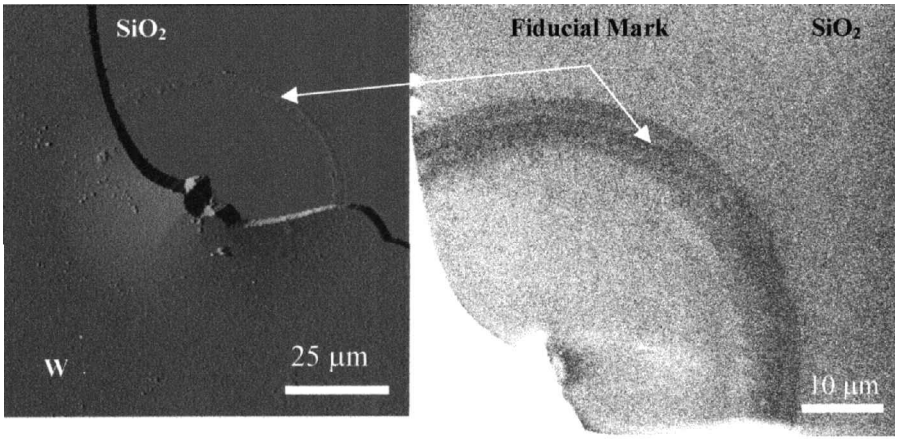

Figure 1. Deflection AFM and SEM images of a partially removed blister, showing the fiducial mark underneath.

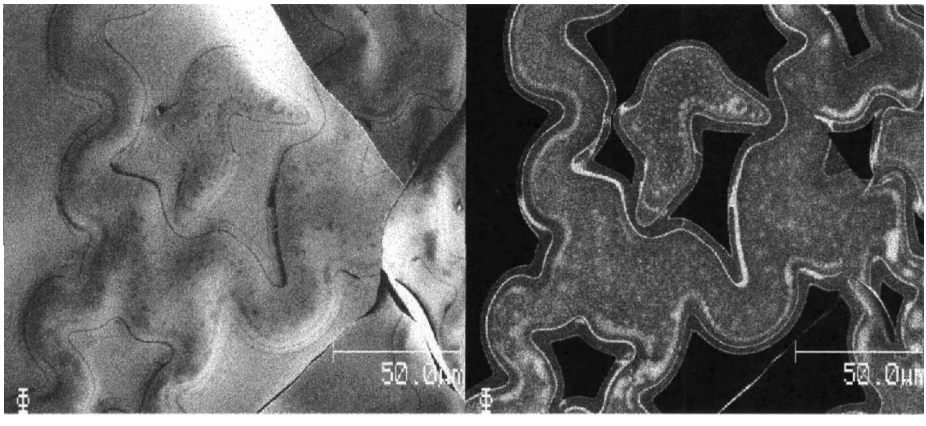

Figure 2. Scanning electron micrograph and corresponding carbon Auger map of a GaAs fracture surface upon TiW_xN_y film removal.

during the film pull-off with the adhesive tape. Most of the carbon goes into the crack tip, outlining the telephone cord topography. Fiducial marks form in conjunction with local film decohesion, with a crack front of the order of 20–200 μm in length. Such marks have not been observed when initially adhered film with no prior delamination goes through an adhesive tape pull-off test.

Radial and interfacial cracking allows laboratory air with moisture, hydrocarbons and surface debris to be sucked into the blisters' crack tip (Volinsky *et al.* 1999a, b 2002a), leaving the fiducial mark detected in figures 1 and 2. Upon blister removal with adhesive tape the crack tip residue splits into two fiducial marks, leaving one on the film and substrate sides as shown in figure 3. The substrate fiducial mark outlines the crack tip geometry, and its dimensions can be used to extract the thin-film crack arrest toughness (Volinsky *et al.* 1999a, b).

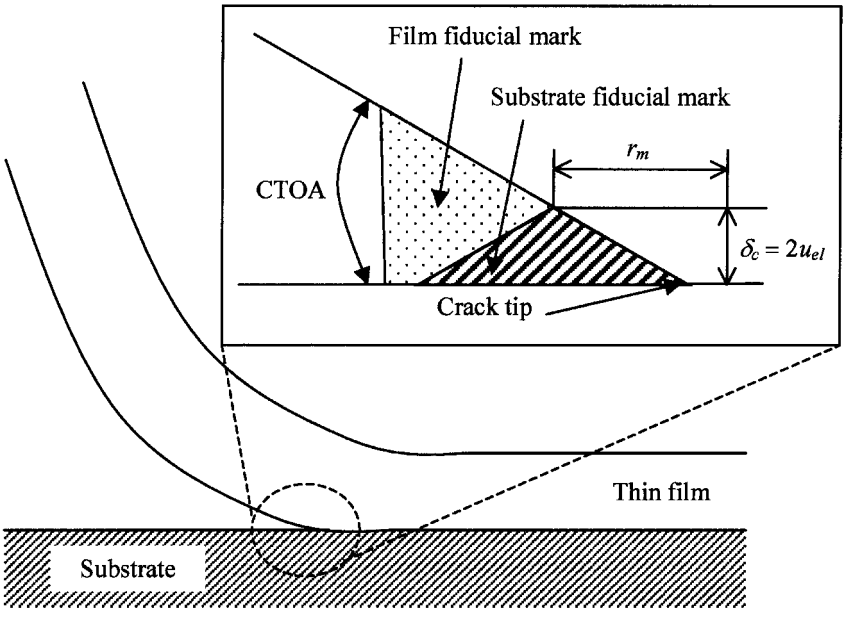

Figure 3. Schematic diagram of the fiducial mark.

§ 3. Elastic crack analysis

As discussed by Volinsky *et al.* (1999b, 2002b) and Tymiak *et al.* (2000), brittle fracture is observed for thinner copper films (less than 120 nm) on silicon substrates. For this case it was desirable to determine how closely the fracture represented linear elastic behaviour. The majority of blisters in these copper films are buckled; so the crack has a significant mode I loading component, which allows one to use the elastic crack-tip-opening displacement expressed for the plane stress tensile loading at a distance r from the crack tip (Lawn 1993):

$$u_{\mathrm{el}}(r) = \frac{K}{E}\left(\frac{8r}{\pi}\right)^{1/2}. \tag{1}$$

AFM measurements of the fiducial mark on the substrate side provide the height $\delta_{\mathrm{c}} = 2u_{\mathrm{el}}(r_{\mathrm{m}})$ and the half-width r_{m} of the mark (figure 3); so K_{I} can be expressed as

$$K_{\mathrm{I}} = \delta_{\mathrm{c}} E\left(\frac{\pi}{32 r_{\mathrm{m}}}\right)^{1/2}. \tag{2}$$

From equation (2), for $\delta_{\mathrm{c}} = 8$ nm and $r_{\mathrm{m}} = 1$ μm (from figure 1), one finds $K_{\mathrm{I}} = 0.3$ MPa m$^{1/2}$. This is close to the 0.33 MPa m$^{1/2}$ value calculated from the actual G measurements (about 0.9 J m^{-2}) for thinner copper films using $K = (GE)^{1/2}$ for plane stress (Volinsky *et al.* 1999b, 2002b, Tymiak *et al.* 2000). Since the analysis is purely elastic, it indirectly proves that there is not much plastic energy dissipation at the crack tip for thin copper films in the brittle-to-ductile transition interval for thicknesses less than 120 nm.

§ 4. Plastic crack analysis

Since the adhesion results considered here are in the region of brittle-to-ductile transition for copper films, allowing very limited plasticity, we previously employed an approach based on the Rice–Drugan–Sham (RDS) analysis of the tearing modulus T_0 (Anderson 1991) to interpret the result (Volinsky *et al.* 1999b).

One can obtain a simple expression for strain energy release rate in terms of the crack-tip-opening angle (CTOA) (in figure 3):

$$J_{SS} = J_0 \exp\left(\frac{\alpha T_0}{\beta}\right) = J_0 \exp\left(\frac{E\ \mathrm{CTOA}}{\sigma_{ys}\beta}\right), \tag{3}$$

where J_0 is the initial value of the J integral at crack initiation, T_0 is the tearing modulus, $\alpha \approx 1$, $\beta = 5.1$ from the mechanics description, and E and σ_{ys} are modulus and yield strength respectively. With an average value of the CTOA of 0.01 rad, a modulus of 120 GPa, a yield strength of 613 MPa (Tymiak *et al.* 2000, Volinsky *et al.* 2002b) and $\beta = 5.1$, one finds that:

$$J_{SS} = J_0 \exp(0.38) \approx 1.47 J_0, \tag{4}$$

which means that during slow crack growth the strain energy release rate has barely increased for this copper film 120 nm thick. This again agrees within experimental error with the actual measured value of about $0.9\ \mathrm{J\,m^{-2}}$ for the strain energy release rate. It may be noted that equations (3) and (4) represent plane-strain behaviour, which seems inconsistent with the thin films evaluated. However, the stress intensity of only $0.33\ \mathrm{MPa\,m^{1/2}}$ in conjunction with a yield strength of 0.61 GPa (Volinsky *et al.* 2002b) represents an experimentally small plastic zone size radius of about 47 nm even if a plane-stress estimate of $K_I^2/2\pi\sigma_{ys}^2$ is used. This only represents about one-third of the film thickness. Even more constraining is the 1 μm superlayer of tungsten with a modulus and yield strength nearly three times that of copper. Given these considerations, we assume that the plastic zone size is best represented by plane strain conditions. These two results in §§ 3 and 4 imply that extremely limited plasticity occurred during the delamination process. To verify this, some dislocation estimates were invoked as follows.

§ 5. Crack renucleation and dislocation shielding

In several focused-ion-beam cross-sections, it was noted that crack growth in the Cu/SiO_2 system was discontinuous. This is seen in figure 4, where separate nucleation events in front of the main circular delamination are present. These 'nanocracks' ranged from 30 to 100 nm in size, spaced anywhere from 50 to 300 nm apart. To consider how this might have occurred we examine the dislocation shielding model of Rice and Thomson (1974), Lin and Thomson (1986) and Thomson (1986) as applied to an embedded thin film. This was first proposed by Hsia *et al.* (1994) for a ductile thin layer embedded between two brittle layers. This is approximately the case here with the copper film bounded by the silicon wafer and the tungsten superlayer. If one estimates the number of shielding dislocations by assuming that the elastic mismatch between a thin Cu and Si/SiO_2 layers is negligible, this was proposed to be

$$n = \frac{4\pi(1-\nu)}{\ln(\tilde{h}/\tilde{r})}\left[\frac{\tilde{K}_{app}\tilde{h}^{1/2}}{A(2\pi)^{1/2}}\sin\varphi\cos\left(\frac{\varphi}{2}\right) - \tilde{\gamma}\right], \tag{5}$$

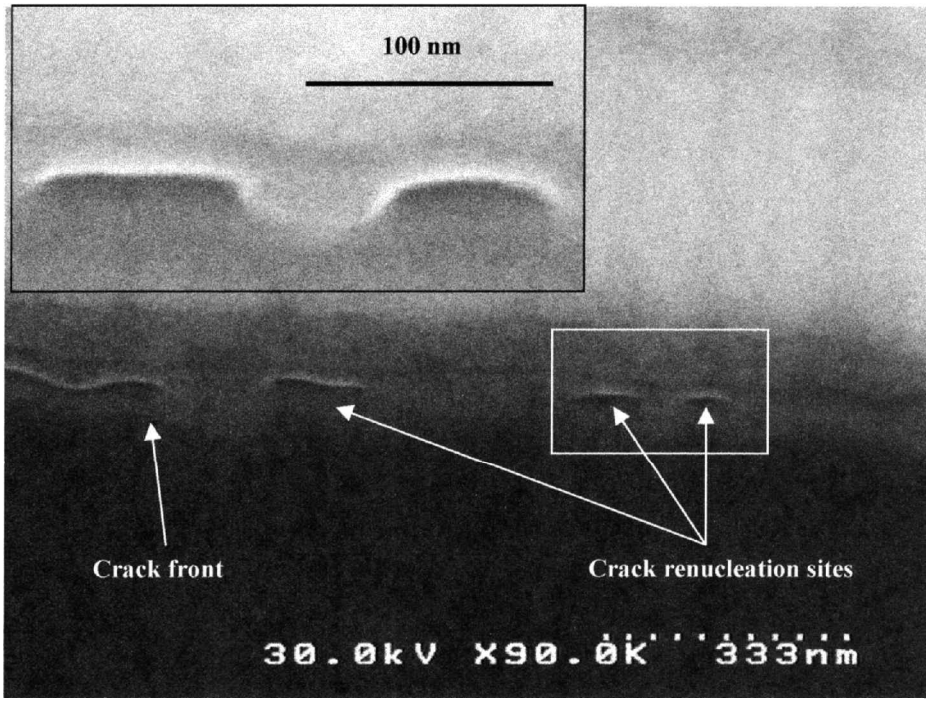

Figure 4. SEM image of the focused-ion-beam cross-section of the crack tip showing crack renucleation.

where ν is Poisson's ratio, φ is the angle between the crack and the slip plane and the tilde quantities are normalized values of thickness $\tilde{h}$, dislocation core $\tilde{r}$, stress intensity $\tilde{K}_{app}$ and surface energy $\tilde{\gamma}$, as given for the case analysed here by:

$$\tilde{h} = \frac{2^{1/2}h}{b}, \quad \tilde{r} \approx 1, \quad \tilde{K} = \frac{K}{\mu b^{1/2}}, \quad A \approx 1, \quad \varphi = 45°, \quad \tilde{\gamma} = \frac{\gamma}{\mu b}. \tag{5a}$$

We have taken the liberty here of assuming the case suggested by a superdislocation approach which gives $\tilde{r} = A = 1$ and have taken the additional liberty of using the full slip band length emanating at the SiO_2–Cu interface and arresting at the Cu–W interface rather than half that as was analysed by Hsia *et al.* (1994) for a cohesive fracture. Using the Rice–Thomson (1986) value of $\tilde{\gamma} = 0.168$ for copper, $\mu_{Cu} = 46$ GPa, $b_{Cu} = 0.255$ nm and $K_{app} = 0.33$ MPa $m^{1/2}$ as observed for the film 120 nm thick, we calculate $n = 4$. This is a reasonable value and agrees with the value reported by Hsia *et al.* (1994) of about four dislocations for $\sigma_c \approx 0.3$, a normalized fracture stress. If these dislocations were equally distributed over the slip plane, they would be spaced 42 nm apart. This value can be further compared with the value of c, the nearest dislocation to the crack tip distance from the Lin–Thomson model. As developed in more detail elsewhere (Gerberich *et al.* 2000, Volinsky *et al.* 2002b) to predict the brittle-to-ductile transition, the shielding model gives

$$K_I^2 = \frac{\sigma_{ys}^2 c}{5.96} \exp\left\{\frac{k_{IG}}{0.76\sigma_{ys}c^{1/2}}\right\}, \tag{6}$$

where k_{IG} is equivalent to $K_I = 0.33\,MPa\,m^{1/2}$ at the lower limit. We have assumed previously that this occurs at or near a thickness of 100 nm (Volinsky *et al.* 1999b, 2002b, Gerberich *et al.* 2000). If we assume here that $K_I = k_{IG}$, the Griffith value, at $h = 120\,nm$, where the yield strength is 613 MPa (Volinsky *et al.* 2002b), this gives a calculated value of $c \approx 31\,nm$. This is sufficiently close to the 42 nm spacing determined above to suggest that these approaches are consistent, noting that they both come from the Rice–Thomson (1974) and the Lin–Thomson (1986) formalism. How might this be used to explain the discontinuous crack patterns noted in figure 4? Firstly, emphasize that this is not an isolated observation. Secondly, while environmental effects cannot be completely eliminated, if the nanocracks are truly isolated, the environmental access would necessarily be by a slower diffusive process. In addition, such cracking could only occur in conjunction with residual stress relief. It is assumed that this was largely removed after delamination and buckling. While leaving this as an option, we at present interpret this discontinuous cracking as a response to the local stress field as perturbed by dislocation emission. Consider the schematic diagram shown in figure 5. The three nanocracks in figure 4 have an average length of 60 nm. The dislocation glide path for a 120 nm film and a 45° slip plane (trace of a {111}) is 170 nm. As suggested by the idealized schematic diagram in figure 5, the four emitted dislocations equally spaced would shield the main crack tip but the tensile stress below the core would reinforce the local stress ahead of the main crack front. We assume that this achieves a maximum local stress at the end of the blocked slip band. This then renucleates a crack at the weakest interface, giving rise to a nanocrack 60 nm long (figure 4). When this occurs three times, a total extended crack zone from the tip of the main crack to the end of the nanocrack of 600 nm results, while the observed length of the zone is 630 nm. This degree of agreement is clearly fortuitous as another example of four renucleation events with 200 nm sized average nanocracks gave a calculated zone of 1080 nm versus an observed value of 1600 nm. These are still sufficiently close that the above-hypothesized scenario has possibilities.

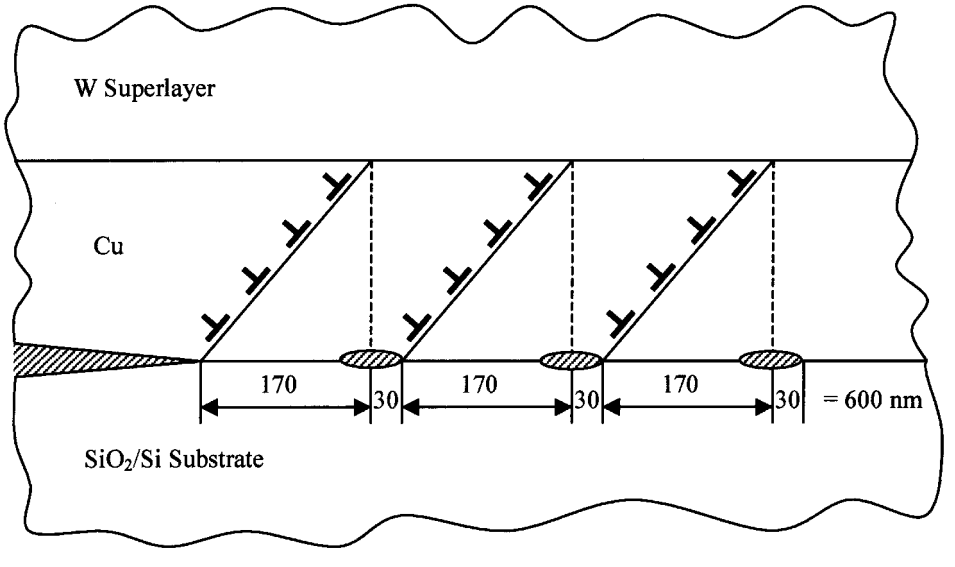

Figure 5. Schematic diagram of the idealized nanocrack zone.

§6. Conclusions

We have shown that fiducial marks formed in thin-copper-film delamination give a good measure of the crack-tip-opening displacement. In turn this can be used to estimate the fracture resistance as verified by the superlayer nanoindentation technique. Both elasticity and tearing modulus estimates of the critical stress intensity agree to first order with an independently measured fracture toughness based on the driving force for crack growth. These results strongly suggest that there was nearly negligible plasticity involved in delaminating this 120 nm film in the lower shelf of the brittle-to-ductile transition. Further corroboration comes from two dislocation shielding analyses, which suggest that only four emitted dislocations are required to account for the present results. This further leads to a reasonable scenario for how a discontinuous nanocrack zone of roughly micron dimensions might form during the arrest of such delaminated films.

Acknowledgements

The authors would like to acknowledge support through US Department of Energy grants DE-FG02/96ER45574 and DE-AC04-94AL85000. We would like to thank Lester Casoose for focused-ion-beam and SEM work. We would also like to acknowledge W. Miles Clift and Bernice E. Mills from Sandia National Laboratories at Livermore for Auger analysis on Cu films, and Robert F. Cook from the University of Minnesota and Joseph B. Vella for valuable discussions.

References

Anderson, T. L., 1991, *Fracture Mechanics: Fundamentals and Applications* (Boston, Massachusetts: CRC Press), p. 219.

Bagchi, A., and Evans, A., 1995, *Mater. Res. Soc. Symp. Proc.*, **383**, 183.

Bagchi, A., Lucas, G., Suo, Z., and Evans, A., 1994, *J. Mater. Res.*, **9**, 1734.

Dauskardt, R. H., Lane, M., Ma, Q., and Krishna, N., 1998, *Engng Fracture Mech.*, **61**, 141.

Gerberich, W. W., Kramer, D. E., Tymiak, N. I., Volinsky, A. A., Bahr, D. F., and Kriese, M., 1999, *Acta mater.*, **47**, 4115.

Gerberich, W. W., Volinsky, A. A., Tymiak, N. I., and Moody, N. R., 2000, *Mater. Res. Soc. Symp. Proc.*, **594**, 351.

Hsia, K. J., Suo, Z., and Yang, W., 1994, *J. Mech. Phys. Solids*, **42**, 877.

Kriese, M. D., and Gerberich, W. W., 1999, *J. Mater. Res.*, **14**, 3007.

Kriese, M. D., Gerberich, W. W., and Moody, N. R., 1999, *J. Mater. Res.*, **14**, 3019.

Lawn, B., 1993, *Fracture of Brittle Solids* (Cambridge University Press).

Lin, I. H., and Thomson, R., 1986, *Acta mater.*, **34**, 187.

Marshall, D. B., and Evans, A. G., 1984, *J. appl. Phys.*, **56**, 2632.

Moody, N. R., Adams, D., Volinsky, A. A., Kriese, M., and Gerberich, W. W., 2000, *Mater. Res. Soc. Symp. Proc.*, **586**, 195.

Moody, N. R., Hwang, R. Q., Venka-Taramani, S., Angelo, J. E., Norwood, D. P., and Gerberich, W. W., 1998a, *Acta mater.*, **46**, 585.

Moody, N. R., Medlin, D., Boehme, D., and Norwood, D. P., 1998b, *Engng Fract. Mech.*, **61**, 107.

Moody, N. R., Medlin, D., Norwood, D. P., and Gerberich, W. W., 1997, *Mater. Res. Soc. Symp. Proc.*, **505**, 97.

Rice, J. R., and Thomson, R., 1974, *Phil. Mag.*, **29**, 73.

Sanchez, J. M., El-Mansy, S., Sun, B., Scherban, T., Fang, N., Pantuso, D., Ford, W., Elizalde, M. R., Martinez-Escanola, J. M., Martin-Meizoso, A., Gil-Sevillano, J., Fuentes, M., and Maiz, J., 1999, *Acta mater.*, **4**, 4405.

Schneider, J. A., Guthrie, S. E., Kriese, M. D., Clift, W. M., and Moody, N. R., 1998, *Mater. Res. Soc. Symp. Proc.*, **522**, 347; 1999, *Mater. Sci. Engng*, **A259**, 253.

Thomson, R., 1986, *Scripta metall.*, **220**, 1473.

Tymiak, N. I., Volinsky, A. A., Kriese, M. D., Downs, S. A., and Gerberich, W. W., 2000, *Metall. Mater. Trans.* A, **31**, 863.
Vlassak, J. J., and Nix, W. D., 1992, *J. Mater. Res.*, **7**, 3242.
Vlassak, J. J., Drory, M. D., and Nix, W. D., 1997, *J. Mater. Res.*, **12**, 1900.
Volinsky, A. A., Clift, W. M., Moody, N. R., and Gerberich, W. W., 1999a, *Mater. Res. Soc. Symp. Proc.*, **586**, 255.
Volinsky, A. A., and Gerberich, W. W., 1999b, *Mater. Res. Soc. Symp. Proc.*, **563**, 75.
Volinsky, A. A, Kottke, M. L., Moody, N. R., and Gerberich, W. W., 2002a, *Engng. Fract. Mech.*, **69**, 1511.
Volinsky, A. A., Moody, N. R., and Gerberich, W. W., 2000a, *Mater. Res. Soc. Symp. Proc.*, **594**, 383.
Volinsky, A. A, Moody, N. R., and Gerberich, W. W., 2002b, *Acta mater.*, **50**, 441.
Volinsky, A. A., Tymiak, N. I., Kriese, M. D., Gerberich, W. W., and Hutchinson, J. W., 1999b, *Mater. Res. Soc. Symp. Proc.*, **539**, 277.
Volinsky, A. A., Vella, J. B., and Gerberich, W. W., 2002c, *Thin Solid Films* (in print).